

Generation of Strong MHD Alfvénic Turbulence

K. Akimoto^(a) and D. Winske

Los Alamos National Laboratory, Los Alamos, New Mexico 87545

(Received 24 July 1989)

Strong Alfvénic turbulence containing a number of solitonlike structures propagating at super-Alfvénic speeds is generated self-consistently and studied by means of computer simulation. A one-dimensional hybrid (kinetic ions, fluid electrons) code is used to investigate the nonlinear evolution of an electromagnetic ion-beam instability that generates low-frequency Alfvén-like waves. As the instability develops, the field-aligned hydromagnetic waves steepen, forming a soliton that bifurcates several times, leading to a fully turbulent state.

PACS numbers: 52.35.Ra, 52.35.Mw, 52.35.Sb, 52.65.+z

The solar wind is a well studied example of magneto-hydrodynamic (MHD) turbulence. The so-called foreshock region upstream of planetary and cometary bow shocks is particularly interesting, as there the level of magnetic field and density fluctuations in the solar wind can be greatly enhanced and various types of nonlinear wave forms^{1,2} (e.g., pulsations, shocklets, hot diamagnetic cavities) are commonly observed. Three diverse, and seemingly unrelated, theoretical methods have been used with some success to model properties of upstream turbulence. One approach extends fluid-turbulence formalisms to magnetized plasmas and often involves spectral MHD calculations to describe the resulting processes in wave-number (k) space.³ A second method employs analytic and numerical solutions of the derivative nonlinear Schrödinger (DNLS) equation to investigate wave-packet steepening and solitary-wave formation.⁴⁻⁶ The third approach uses linear, quasilinear, and nonlinear theory to interpret the results of hybrid (particle ions, massless fluid electrons) simulations that follow the growth and evolution of electromagnetic waves.⁷ In this paper we report the results of a one-dimensional hybrid simulation in which strong Alfvén turbulence is generated self-consistently. The turbulence is characterized by solitonlike structures and shows evidence of a nonlinear cascade of Alfvén-like waves. The calculation thus displays features associated with each of the three methodologies.

The turbulence is generated by an electromagnetic ion-beam instability due to the streaming of a tenuous, field-aligned ion beam (density $n_b/n_e = 0.015$) relative to the background ions (density n_m) with speed $v_0 = 10v_A$ ($v_A =$ Alfvén speed) in the presence of a charge-neutralizing electron background (electron density $n_e = n_b + n_m$). These parameters are similar to those in the Earth's foreshock, where the ambient ions correspond to the solar-wind protons and the beam ions to the protons reflected from the bow shock.¹ The simulations are carried out with an electromagnetic hybrid code in a manner very similar to that described in Ref. 7, except that here the plasma beta [$\beta =$ ratio of plasma pressure

(based on the electron density) to the magnetic pressure] is 0.2 for all species (instead of 1.0), the spatial resolution is much better [cell size $\Delta x = 0.5c/\omega_i$ (ion inertia length), instead of 2.0], with a correspondingly smaller time step, $\Omega_i \Delta t = 0.005$ ($\Omega_i =$ proton cyclotron frequency), and an improved predictor-corrector method with no phenomenological resistivity included is used to solve the radiationless Maxwell equations. As before,⁷ the system length is $256c/\omega_i$ and the electron temperature $T_e = \text{const.}$

As the simulation proceeds, the proton beam first becomes unstable to the electromagnetic ion-ion resonant instability,⁸ and generates low-frequency ($\omega_r \ll \Omega_i$), large-amplitude ($\delta B \leq B_0$), right-circularly polarized waves, where ω_r is the real wave frequency, δB is the fluctuating magnetic field amplitude, and B_0 is the strength of the external magnetic field. Rigorously speaking, these waves are beam-mode waves connected to the whistler-magnetosonic branch, which corresponds to the MHD slow-mode branch in a low- β plasma.⁴ These waves typically have a group velocity of $\sim v_0/2 = 5v_A$. As the beam is scattered by the waves, the dispersion relation of the waves approaches that of Alfvén or slow MHD waves. Figure 1(a) displays profiles of the total ion density n , the magnetic field fluctuations $\delta B = (B_y^2 + B_z^2)^{1/2}$, and the two transverse field components, B_y and B_z , at about the time when the total magnetic-field-fluctuation level saturates. One sees from the bottom two panels that the waves are circularly polarized and that modes 4 and 5 dominate, consistent with linear theory, as are the measured linear growth rates. Figure 2(b) shows the system somewhat later in time. While evidence for circular polarization and remnants of modes 4 and 5 can still be seen, it is clear that shorter-wavelength waves have also grown up. By the end of the simulation, the proton beam has given up approximately one-third of its initial energy, of which 40% goes into wave energy and 60% into thermal energy of the ambient ions. To this level of description the third methodology gives a good account of the evolution of the system.

On the other hand, if one instead concentrates on the

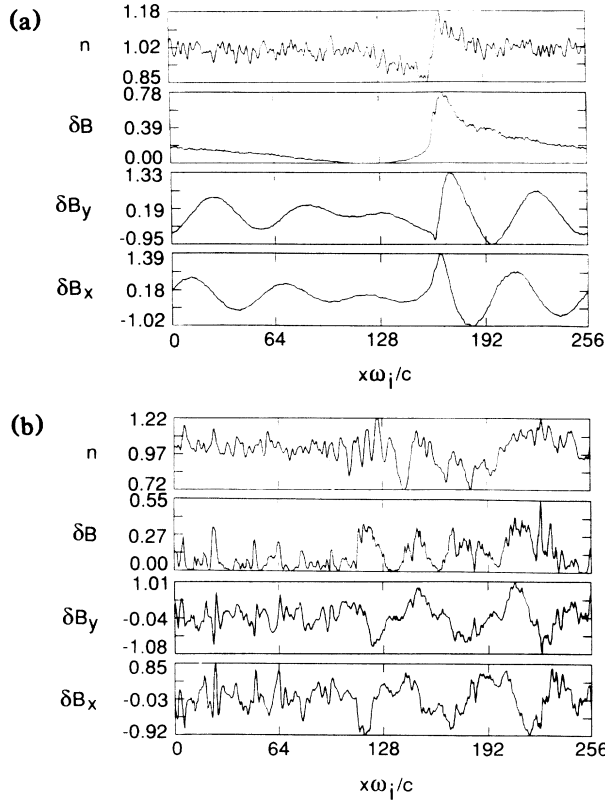


FIG. 1. From top to bottom: n , δB , δB_y , and δB_x as a function of $x/(c/\omega_i)$ at $\Omega_i t$ equal to (a) 45 and (b) 75.

steepening of the density and the magnitude of the magnetic field fluctuations, another perspective can be obtained. From the top panels in Fig. 1(a), namely n and δB , it is evident that even during the period of linear growth, dramatic nonlinear effects are taking place. By beating, the modes 4 and 5 form a wave packet at $\Omega_i t \sim 30$, the trailing end of which steepens and forms a solitonlike structure about the time of saturation $\Omega_i t \sim 45$. Since this and other nonlinear wave packets that form are qualitatively similar to Alfvén solitons,^{5,6} we shall refer to them as solitons. However, all of these entities are not solitons in a mathematically rigorous sense, because some of them collapse. We further note in Fig. 1(a) the positive correlation between the density enhancement and the soliton as well as the density cavity at its immediate left.

The evolution of the steepening or collapsing soliton is depicted in Fig. 2(a). Displayed are profiles of δB for the period $0 < \Omega_i t < 50$ (the separation between profiles is $\Omega_i t = 1$). Also observable at later time is the bifurcation of the primary soliton into two second-generation solitons with super-Alfvénic velocities, $v = 2.4v_A$ and $-2.2v_A$, in the electron (zero-current) frame of the simulation. Figure 2(b) displays a similar plot with a compressed scale for the fluctuating magnetic field during the entire simulation. It is clearly seen that the

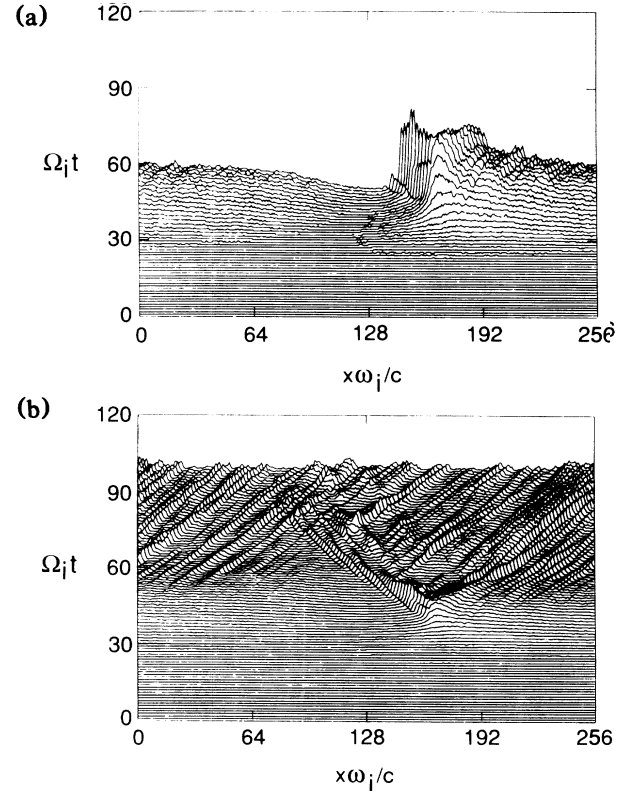


FIG. 2. Profiles of the fluctuating magnetic field δB as a function of $x/(c/\omega_i)$ and $\Omega_i t$ for the durations of (a) $0 < \Omega_i t < 50$ and (b) $0 < \Omega_i t < 80$, with different scales for δB .

second-generation soliton with negative velocity bifurcates again at $\Omega_i t \sim 47$. This bifurcation is observed to then occur many more times. All of these bifurcating solitons have almost identical speeds $v \sim \pm 2.4v_A$. In addition, while the trailing end of the initial wave packet collapses, the weakly modulated portion breaks up and also forms solitons. These solitons do not bifurcate, but also have a constant speed of $v \sim 1.6v_A$. By $\Omega_i t \sim 80$, the bifurcation stops, and well developed Alfvén turbulence, composed of many solitons and quasisolitons with positive velocities, results. Given this picture of the temporal evolution of the solitary-wave structures, the complexities of Fig. 1(b) become clearer. For example, the peaks in δB at $x/(c/\omega_i) = 25, 50, 64$ are nonbifurcating solitons. At $x/(c/\omega_i) \sim 120$ there is a quasisoliton, which is a product of bifurcation, while at $x/(c/\omega_i) \sim 230$ two nonbifurcating solitons have emerged from a second-generation soliton with positive velocity.

To show that these wave packets have soliton properties, recall that solitons are nonlinear, coherent solitary pulses, the functional form of which is given by⁴⁻⁶ $f(kx - \omega t)$, where $k(\omega)$ is the characteristic wave number (frequency) of solitons. Thus, a soliton has a constant velocity ω/k , as the simulation has demonstrated. Second, in the soliton's frame of reference, the phase should remain constant. It has been shown that this is

true for the primary (collapsing) soliton, the second-generation bifurcating solitons, and the nonbifurcating solitons. There are, however, other bifurcating solitons that do not have constant phases. Finally, while the primary soliton has a characteristic half-width of $15c/\omega_i$, the other solitons typically have half-widths of $(2-3)c/\omega_i$ or 4-6 ion gyroradii.

To place these results in the context of earlier work,⁴⁻⁶ we note that the DNLS equation is basically valid only for weak Alfvén turbulence in which $\delta B \ll B$, in contrast to the situation here ($\delta B \sim B$ at $\Omega_i t \leq 50$). Furthermore, the DNLS equation is based on the usual Alfvén wave rather than the beam-modified mode that is excited by the ion-beam instability. Also, dissipation of Alfvén waves is absent in the DNLS equation. In addition, the wave steepening and collapse is not entirely due to wave-wave interactions, as assumed in the DNLS equation. As shown recently by Terasawa,⁹ the steepening causes the deceleration of beam ions, locally forming clumps. It is possible for these clumps to further excite Alfvén-like waves. In spite of these differences, the DNLS equation does describe the primary-soliton collapse⁶ (if $\beta > 1$), similar to that observed in the simulations, although $\beta < 1$ here. It should also be noted that Omura and Matsumoto¹⁰ have recently discovered a mechanism for generating a backscattered wave from a right-circularly polarized wave. Such a mechanism seems promising in explaining the bifurcation of the solitons.

Figure 3 shows Fourier spectra $|\delta B_y(k)|^2/B_0^2$ at various times in the run. In Fig. 3(a) we observe the presence of the two dominant modes (4,5) generated by the instability, while Fig. 3(b) shows cascading of the pump waves to a higher wave number. The spectrum obeys a

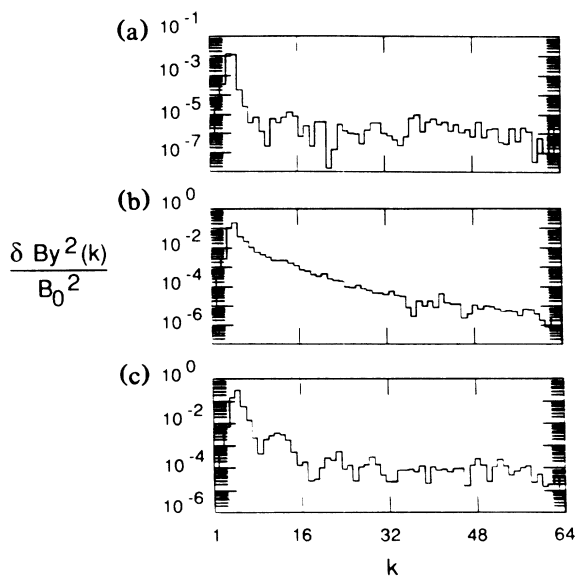


FIG. 3. Fourier spectra $|\delta B_y(k)|^2/B_0^2$: (a) $\Omega_i t = 30$, (b) $\Omega_i t = 40$, and (c) $\Omega_i t = 50$.

power law with a power-law index of about 4.5. This is in contrast to the exponential spectra predicted by the DNLS equation.⁶ Finally, at later times [Fig. 3(c)] the spectrum exhibits harmonics.

While we have shown here only one example of soliton formation, a number of simulations have been performed. Holding the beam velocity constant, the primary-soliton collapse has been observed for the beams with densities $0.005 \leq n_b/n_e \leq 0.025$. The entire scenario is repeated in plasmas with higher total β . From these runs we conclude that the strong Alfvén turbulence described here possesses the following properties, which are not shared by weak Alfvén turbulence:⁴⁻⁶ (1) the primary-soliton collapse of a right-circularly polarized wave packet occurring even in a plasma with low $\beta = 0.4 < 1$, (2) the presence of bifurcating solitons, and (3) the positive correlation between δB and δn at both $\beta < 1$ and $\beta > 1$.

To relate these results to the more formal description of MHD turbulence,¹ we note that the source of the Alfvén-like turbulence is the electromagnetic ion-ion instability and that the sink is provided by solitons. As shown above, the inertial range between the source and sink has a power-law relationship. This is consistent with Ref. 3, although such a comparison is obviously more meaningful in a continuously driven system. A more detailed comparison is in progress.

In conclusion, the simulations have demonstrated that field-aligned Alfvén-like MHD waves steepen and become compressible, leading to well developed Alfvén turbulence containing a number of solitons. Evidently, more work is needed to further understand this strongly turbulent state and to draw together the three methodologies. This will include more extensive parametric studies of the initial conditions $(n_b/n_e, v_0, \beta)$, the wave propagation angle with respect to \mathbf{B}_0 , and the two-dimensional effects. While the basic properties of the hydrodynamic waves are similar in 2D,¹¹ one expects the nonlinear behavior to be more complex, as many more wave-wave interactions are possible. In addition, the interaction of the solitons with both the beam and background ions to produce localized regions of dissipation, contrary to the usual quasilinear diffusion picture,⁷ requires more study. Finally, the relation of these entities to the rich dataset of observations of solitonlike structures in the Earth's foreshock^{1,2} needs to be investigated further.

The authors would like to thank S. P. Gary and M. F. Thomsen for useful conversations. One of the authors (K.A.) is supported by NASA Grant No. W-17,002. This work was performed under the auspices of the U.S. Department of Energy.

(a) Now at Department of Electrical and Electronic Systems Engineering, Teikyo University, Utsunomiya 320, Japan.

¹M. M. Hoppe, C. T. Russell, L. A. Frank, T. E. Eastman,

and E. W. Greenstadt, *J. Geophys. Res.* **86**, 4471 (1981).

²M. F. Thomsen, J. T. Gosling, S. J. Bame, and C. T. Russell, *J. Geophys. Res.* (to be published).

³A. F. Viñas, M. L. Goldstein, and M. H. Acuña, *J. Geophys. Res.* **89**, 3762 (1984).

⁴A. Hasegawa and C. Uberoi, *The Alfvén Wave* (Technical Information Center, U.S. Department of Energy, Washington, DC, 1982).

⁵E. Mjølhus and J. Wyller, *Phys. Scr.* **33**, 442 (1985).

⁶S. R. Spangler, *Astrophys. J.* **299**, 122 (1985).

⁷D. Winske and M. Leroy, *J. Geophys. Res.* **89**, 2673

(1984).

⁸S. P. Gary, W. C. Smith, M. A. Lee, M. L. Goldstein, and D. W. Forslund, *Phys. Fluids* **27**, 1852 (1984); **28**, 438(E) (1985).

⁹T. Terasawa, *Comput. Phys. Commun.* **49**, 193 (1988).

¹⁰Y. Omura and H. Matsumoto, in *Plasma Waves and Instabilities at Comets and in Magnetospheres*, edited by B. T. Tsurutani and H. Oya, AGU Monograph No. 53 (American Geophysical Union, Washington, DC, 1988), p. 51.

¹¹D. Winske and K. B. Quest, *J. Geophys. Res.* **91**, 8789 (1986).